UNIVERSITY OF PARDUBICE

FACULTY OF CHEMICAL TECHNOLOGY

Department of Inorganic Technology

Lenka Durčíková

Synthesis and study of hydroxyapatite for pigments purposes

Theses of the Doctoral Dissertation

Pardubice 2021

Study program: **Chemistry and Chemical Technology**

Study field: **Inorganic Technology**

Author: **Lenka Durčíková**

Supervisor: **prof. Ing. Petra Šulcová, Ph.D.**

Year of the defence: 2021

References

DURČÍKOVÁ, Lenka. *Synthesis and study of hydroxyapatite for pigments purposes.* Pardubice, 2021. 153 pages. Dissertation thesis (PhD.). University of Pardubice, Faculty of Chemical Technology, Department of Inorganic Technology. Supervisor Prof. Ing. Petra Šulcová, Ph.D.

Abstract

The presented dissertation thesis deals with the determination of the influence of suitable synthesis conditions by precipitation method (Ca/P ratio; pH; precipitation rate) on the synthesis of hydroxyapatite, in which part of calcium ions was replaced by other ions of selected elements (magnesium, zinc, aluminium and strontium). This was followed by the evaluation of the adaptation of the partial replacement of calcium ions by selected elements in the hydroxyapatite structure and their subsequent characterization by available laboratory techniques (optical and electron microscopy, X-ray diffraction analysis, spectroscopic methods and corrosion tests).

Abstrakt

Předkládaná dizertační práce se zabývá zjištěním vlivu vhodných syntézních podmínek metodou srážení (poměr Ca/P; pH; rychlost srážení) na syntézu hydroxyapatitu, u kterého byla část vápenatých iontů nahrazena jinými ionty vybraných prvků (hořčík, zinek, hliník a stroncium). Dále následovalo vyhodnocení adaptace částečného nahrazení vápenatých iontů zvolenými prvky ve struktuře hydroxyapatitu a jejich následná charakterizace dostupnými laboratorními technikami (optická a elektronová mikroskopie, rentgenová difrakční analýza, spektroskopické metody a korozní zkoušky).

Keywords

Inorganic pigments, corrosion, phosphate pigments, hydroxyapatite, precipitation, substitution, X-ray diffraction, particle size distribution, corrosion test

Klíčová slova

Anorganické pigmenty, koroze, fosforečnanové pigmenty, hydroxyapatit, srážení, substituce, rentgenová difrakce, distribuce velikosti částic, korozní test

TABLE OF CONTENTS

1 INTRODUCTION

Among the group of calcium orthophosphates, hydroxyapatite (hydroxylapatite, HA, HAP) has become the most studied phosphate, where due to its excellent biocompatibility and bioactivity, its considerable attention is concentrated especially in the medical field (orthopaedics, ophthalmology), where these compounds are intended to partially or completely replace bone tissue. A considerably interesting application of hydroxyapatite is its use as a coating for metal prostheses, which has two important functions, namely to protect the incorporated material in the body from corrosion, so that the incorporated materials (e.g. prostheses, implants) have a better, suitable and recognizable surface in the tissue, due to their physicochemical properties and biocompatibility, and the acceptability and inertness of the implanted material towards the human body. Since hydroxyapatite is very suitable for the protection of incorporated implants by preventing corrosion processes both in terms of structural and physicochemical properties, there is a high probability of its usefulness for the protection of steel. As this consideration has not been studied in detail before, it has become the main focus of the present dissertation.

2 THE AIM OF THESIS

The aim was to investigate and evaluate the effect of the synthesis conditions by precipitation method for obtaining and forming hydroxyapatite powder materials. Another objective was to study the partial substitution of calcium ions in the hydroxyapatite structure by other selected elements and its subsequent characterization and description of the physicochemical properties of the pure and doped hydroxyapatite phase by available laboratory techniques (optical and electron microscopy, X-ray diffraction analysis, spectroscopic methods and corrosion tests). Finally, the influence of precipitation conditions and partial substitution by other selected elements on the corrosion inhibiting effect of hydroxyapatite was verified and subsequently evaluated.

3 THEROTETICAL PART

Anti-corrosion pigments (phosphate pigments) belong to the group of special inorganic pigments. They are characterized as powdery substances, most often inorganic in nature, which, when applied to the binders of coating systems, exhibit anticorrosive effects, thus limiting the rate of corrosion of the metal surface [1-3]. The basic principle of action of these pigments is to retard or stop the electrochemical reaction. The main reason for the widespread use of anticorrosive pigments today is the stricter hygienic and environmental limits that appeal to replace toxic lead and chromate pigments with non-toxic but highly effective pigments [4].

Hydroxyapatite ($Ca_{10}(PO_4)_6(OH)_2$; HAP) is the most common phosphate apatite, which has been extensively studied from theoretical and experimental points of view because it is an important biotechnological, technological and industrial element [5, 6]. The general formula for apatite-type compounds is $M_{10}(XO_4)_6Z_2$, where for the hydroxyapatite structure, M is Ca^{2+}, X is P^{5+} and the Z position is represented by the hydroxyl group OH^- [7-10]. Hydroxyapatite occurs in two different crystallographic modifications - hexagonal and monoclinic. The hexagonal system belongs to the $P6_3/m$ space group, which is characterized by hexagonal rotational symmetry and planar reflection with lattice parameters a = b = 0.942 nm and c = 0.689 nm. The monoclinic system is characterized by the space group $P2_1/b$ with lattice parameters a = 0.980 nm, b = 0.200 nm and c = 0.688 nm [11, 12]. The basic crystal modifications of hydroxyapatite are shown in Figure 1.

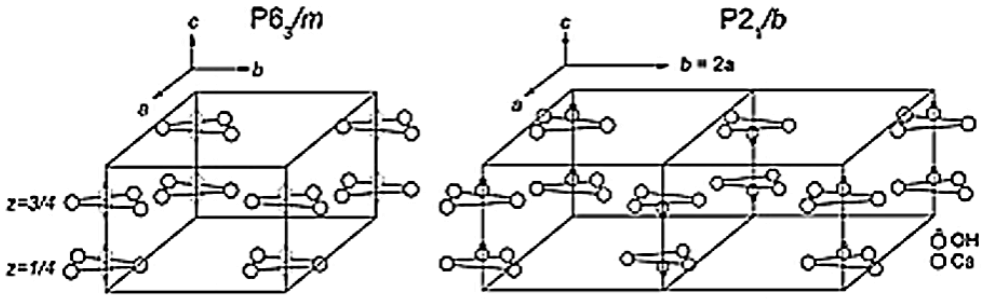

Fig. 1: Crystallographic modification of hydroxyapatite [11, 13]

Monoclinic hydroxyapatite system is more ordered, thermodynamically stable and is constructed with a series of phosphate ions located along the axis and with calcium ions and hydroxyl ions located between the phosphate groups [11, 14]. The hexagonal crystallographic system is most commonly found in natural apatites. Its structure is very similar to the monoclinic HAP system, but the calcium series and hydroxyl groups are located in parallel bands. Ionic substitutions occur more readily in these bands, which may indicate various changes in the structure of natural apatites. In the hexagonal structures of HAP, the hydroxyl groups are in comparison the monoclinic form outside each layer are more disordered and oriented alternately up and down in the structure. These detected stresses are replaced by ionic vacancies or substitutions. Stoichiometric HAP is demonstrated by a calcium to phosphorus atomic ratio of 1.67 (10/6) [14, 15].

In the present work, the influence of suitable synthesis conditions by precipitation method (Ca/P ratio; pH; precipitation rate) on the synthesis of hydroxyapatite, partial substitution of calcium ions in the hydroxyapatite structure by other selected elements (magnesium, zinc, aluminium, strontium) and subsequent evaluation of their possible adaptation in the hydroxyapatite structure is studied.

4 EXPERIMENTAL PART

In order to select and determine the appropriate laboratory synthesis conditions for the formation of pure hydroxyapatite, the thermodynamic stability of the hydroxyapatite phase in an aqueous system under normal laboratory conditions was investigated [16]. Powdered hydroxyapatite samples in three molar ratios of Ca/P =1, 1.67 and 3 were synthesized by precipitation method and subsequently studied at pH = 7 and 12. From previous thesis work [17], the effect of precipitation conditions on the synthesis and structure of hydroxyapatite has already been demonstrated, therefore, the following synthesis conditions were selected for further investigation based on these laboratory results: Ca/P ratio = 1, pH = 7 and precipitation rate = 2 $ml \cdot min^{-1}$, which were applied for the synthesis of doped hydroxyapatite (Table 1). For the synthesis of the samples, 1 $mol \cdot l^{-1}$ solutions of the starting compounds ($Ca(NO_3)_2 \cdot 4H_2O$, $Al(NO_3)_3 \cdot 9H_2O$, $Mg(NO_3)_2 \cdot 6H_2O$, $Zn(NO_3)_2 \cdot 6H_2O$, $Sr(NO_3)_2$, $(NH_4)H_2PO_4$) were prepared, where the exact concentration of these starting materials was determined by selected analytical methods (titration, photometric and gravimetric analyses) [16, 18].

Table 1: Overview of obtained samples and synthesis conditions

Sample	**Phase composition**	**Ratio (Ca+M)/P**	**pH**	**Precipitation rate [$ml \cdot min^{-1}$]**
1	$Ca_{10}(PO_4)_6(OH)_2$	1	7	2
1-Mg	$Ca_{9.5}Mg_{0.5}(PO_4)_6(OH)_2$	1	7	2
1-Zn	$Ca_{9.5}Zn_{0.5}(PO_4)_6(OH)_2$	1	7	2
1-Sr	$Ca_{9.5}Sr_{0.5}(PO_4)_6(OH)_2$	1	7	2
1-Al	$Ca_{9.25}Al_{0.5}(PO_4)_6(OH)_2$	0.975	7	2
2	$Ca_{10}(PO_4)_6(OH)_2$	1.67	7	2
3	$Ca_{10}(PO_4)_6(OH)_2$	3	7	2
4	$Ca_{10}(PO_4)_6(OH)_2$	1.67	12	2

The obtained hydroxyapatite powders were prepared by the synthesis method of precipitation of calcium nitrate tetrahydrate ($Ca(NO_3)_2 \cdot 4H_2O$), which was heated to a temperature of 50-70 °C and ammonium dihydrogen phosphate ($(NH_4)H_2PO_4$) was gradually added using an automatic titrator. An aqueous ammonia solution was used

to adjust the reaction medium to pH 7, and this value of the stirred solution was monitored and measured throughout the synthesis using a pH meter. After mixing of the starting compounds, the analysis of the samples was subsequently carried out by optical microscopy. This was followed by the maturation of the prepared samples for 24 hours, after which the samples were again analysed by optical microscope and the particle size distribution was also measured by Mastersizer. This was followed by filtration, washing with distilled water, drying (80 °C for 6 hours) and sieving of the samples. The obtained synthesized powders were further evaluated for their phase composition (XRD, Rigaku MiniFlex 600), morphology (SEM, Tescan LYRA 3) and corrosion inhibition properties (preliminary and accelerated corrosion tests) [19-23].

5 RESULTS AND DISSCUSION

5.1 Effect of partial substitution on the structure and properties of HAP

Based on the previously investigated synthesis conditions for hydroxyapatite phase formation, sample 1 was selected for partial substitution with selected elements (Mg, Zn, Al, Sr), which was laboratory prepared under the following synthesis conditions: Ca/P ratio = 1 and pH = 7. The synthesized samples were further evaluated in terms of crystal size and morphology (OM, SEM), particle size distribution (PSD), phase composition (XRD) and thermal stability (TG) [20, 23].

5.1.1 Particle size distribution of hydroxyapatite

The following analysis concerns the particle size distribution of the synthesized samples. The signal evaluation was performed using Mie scattering and the distribution curves and the values of d_{10}, d_{50}, d_{90} and the spread of the distribution (span) were obtained. The volume distribution curves of synthesized samples 1 (undoped), 1-Mg, 1-Zn, 1-Al and 1-Sr are shown in Figure 2 for illustration. The width of the distribution range is in the particle size range from 0.45 to 150 µm [20, 23].

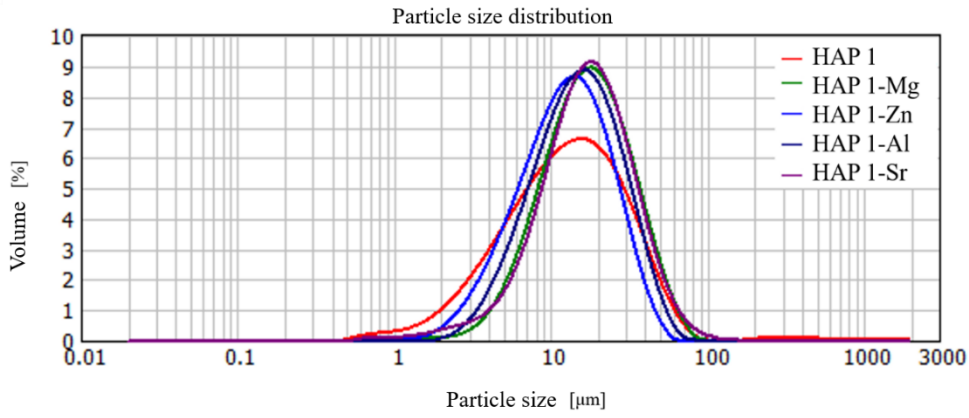

Fig. 2: Distribution curves of synthesized doped samples

Table 2 shows the particle size values (d_{10}, d_{50}, d_{90}) and the span of the measured samples. The results correspond to the size of the agglomerates. The values in the table show that the narrowest particle size distribution was obtained for undoped

sample 1, while doping the sample caused the range of particle size distribution to widen. Sample 1-Mg showed the narrowest range of particle size distribution under substitution, which may be related to the results from XRD analysis, where its two-phase composition was demonstrated, as whitlockite was identified along with hydroxyapatite [20, 23].

Table 2: Overview of the particle size distribution range of synthesized samples

Particle size distribution				
Sample	d_{10} [µm]	d_{50} [µm]	d_{90} [µm]	span
1	3.52	9.80	22.43	1.93
1-Mg	4.97	13.07	27.67	1.74
1-Zn	5.66	17.47	38.99	1.91
1-Al	6.98	14.28	33.15	1.83
1-Sr	6.65	17.13	38.80	1.87

5.1.2 Phase composition of hydroxyapatite

The phase composition of the prepared samples was determined by XRD analysis. Most of the samples showed only single phase composition, but only one doped sample 1-Mg ($Ca_{9.5}Mg_{0.5}(PO_4)_6(OH)_2$) contained two phases, namely hydroxyapatite $Ca_{10}(PO_4)_6(OH)_2$ and whitlockite $Ca_{18}Mg_2H_2(PO_4)_{14}$ (Figure 3, Table 3). As only the hydroxyapatite phase was identified in the other doped samples, it was clear that these doped ions (Zn^{2+}, Al^{3+} and Sr^{2+}) probably occupied the calcium positions in the hydroxyapatite crystal structure. This was expected because the ionic radii of these substituted ions are approximately the same size or smaller than the radius of r (Ca^{2+}) = 0.11 nm (r (Mg^{2+}) = 0.072 nm, r (Zn^{2+}) = 0.074 nm, r (Al^{3+}) = 0.054 nm, r (Sr^{2+}) = 0.13 nm) [20, 23].

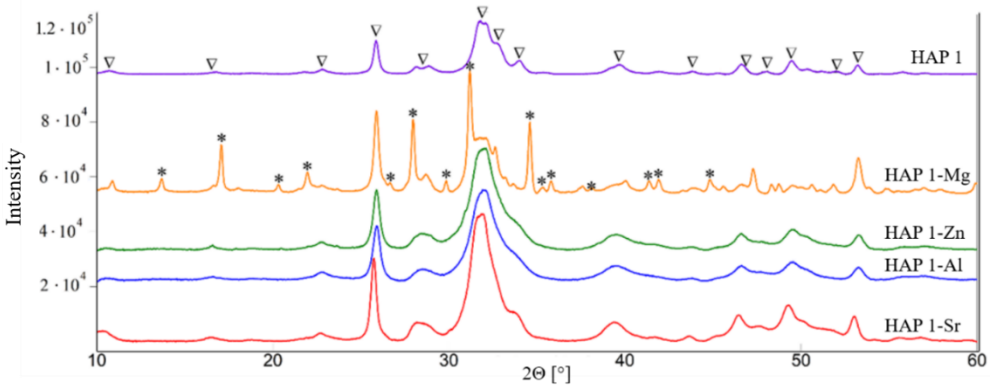

Fig. 3: Diffractogram of undoped and doped hydroxyapatite phase

Table 3: Phase composition of identified hydroxyapatite phases

Sample	Chemical formula	Identified phases
1	$Ca_{10}(PO_4)_6(OH)_2$	$Ca_{10}(PO_4)_6(OH)_2$ (∇, hydroxyapatite)
1-Mg	$Ca_{9.5}Mg_{0.5}(PO_4)_6(OH)_2$	$Ca_{10}(PO_4)_6(OH)_2$, $Ca_{18}Mg_2H_2(PO_4)_{14}$ (*, whitlockite)
1-Zn	$Ca_{9.5}Zn_{0.5}(PO_4)_6(OH)_2$	$Ca_{10}(PO_4)_6(OH)_2$
1-Sr	$Ca_{9.5}Sr_{0.5}(PO_4)_6(OH)_2$	$Ca_{10}(PO_4)_6(OH)_2$
1-Al	$Ca_{9.25}Al_{0.5}(PO_4)_6(OH)_2$	$Ca_{10}(PO_4)_6(OH)_2$

5.1.3 Hydroxyapatite crystal sizes and morphology

By comparing the crystal size results obtained from SEM and XRD analysis, it was found that the minimum sizes from SEM analyses were comparable to the maximum sizes from XRD analyses. In general, the SEM analysis depicts bulkier particles. This phenomenon can be explained by the fact that the largest particles that were visible from SEM were selected for the maximum crystal size analysis (Figure 4). Another explanation was the fact that the largest particles visible in the SEM images were made up of smaller crystals [20, 23].

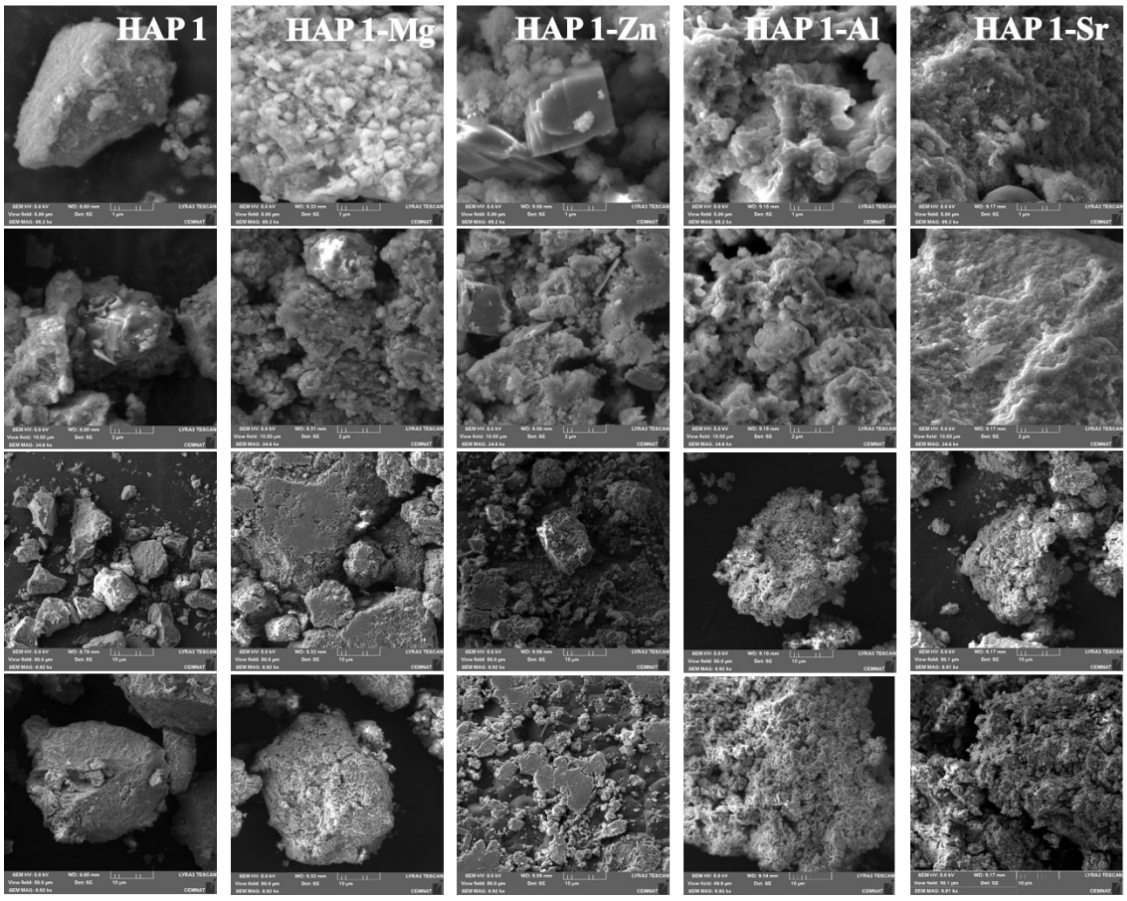

Fig. 4: SEM of undoped and doped HAP samples

5.2 Effect of calcination on the structure of doped hydroxyapatite

The prepared doped hydroxyapatite pigments were calcined at firing temperatures of 800, 1000, 1100 and 1200 °C for 5 h in a calcination furnace and subsequently subjected to PSD, XRD, SEM and EDS analyses.

5.2.1 Particle size distribution of calcinated doped hydroxyapatites

From the measured particle size distribution, the effect of calcination temperature on the size and its distribution of the prepared doped hydroxyapatite powders was investigated. Figure 5 shows the distribution curves of undoped (sample 1) and doped hydroxyapatite samples (1-Mg, 1-Zn, 1-Al, 1-Sr) which were subsequently subjected to calcination at the selected firing temperatures [20, 22, 23].

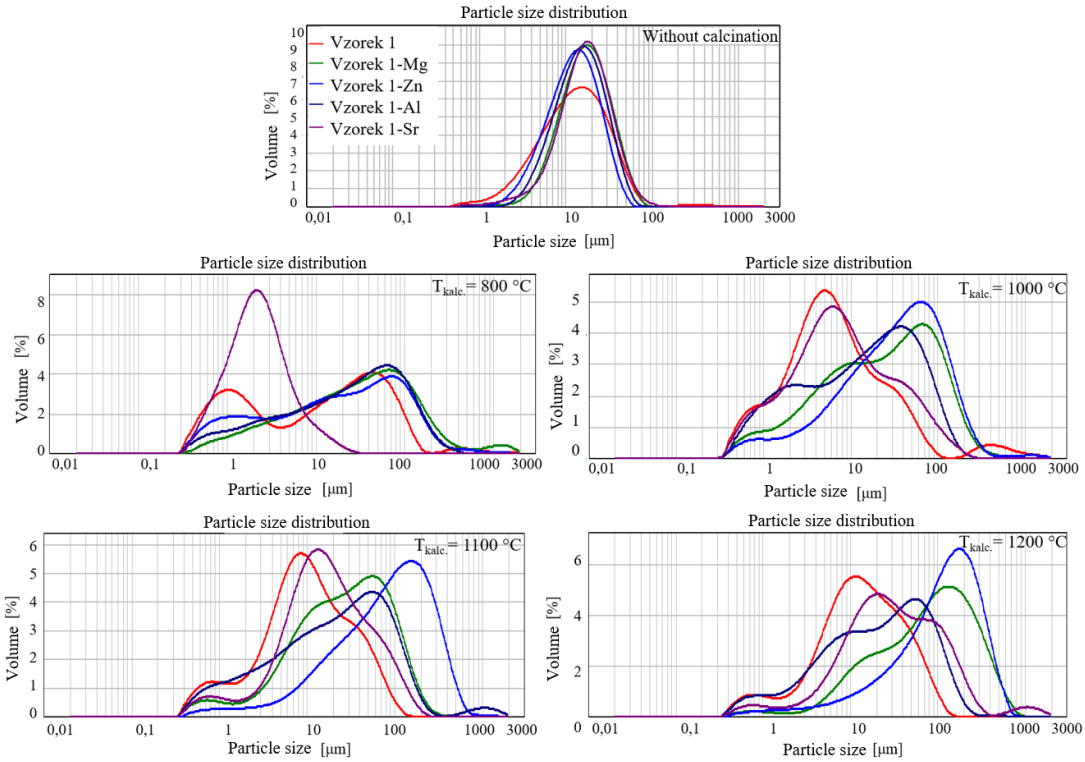

Fig. 5: Distribution curves of doped synthesized samples before and after subsequent calcination ($T_{calc.}$= 800, 1000, 1100 and 1200 °C)

For the measured doped calcined samples, the d_{10} value ranges from 0.77 to 16.52 µm, the d_{50} value ranges from 2.18 to 120.94 µm, and the d_{90} value ranges from 16.27 to 332.76 µm. The range of distribution of the measured samples is from 2.61 to 7.09. From the obtained particle size values, it is clear that the same trend as for undoped samples occurs, i.e., that with increasing firing temperature, the values

of d_{10}, d_{50}, d_{90} increase and, on the contrary, the value of the range of distribution (span) decreases. Higher values of d_{50} and d_{90} were obtained for some samples, which may be due to the presence of a higher proportion of small particles in the total volume and the presence of agglomerates of larger particles, which could be explained by the short dispersion time in the ultrasonic bath. The width of the particle size distribution for the non-calcined doped samples ranges from 0.3 to 100 µm, while for the calcined doped samples the value ranges from 0.3 to 1000 µm. Therefore, from the width of the particle size distribution, it can be concluded that during the firing process, the number of small particles in the total volume decreases, resulting in the formation of agglomerates of larger particles, as evidenced by the width of the distribution curve moving towards higher values [20, 22, 23].

5.2.2 Phase analysis of calcinated doped hydroxyapatite powders

For the synthesized calcined doped samples, the effect of firing temperature in the range of 800-1200 °C on their phase composition was analyzed. The powders were examined by X-ray diffraction analysis, where the PDX 2 database was used to evaluate the phases found. Figure 6 shows the diffractograms of calcined hydroxyapatites doped with Mg^{2+}, Zn^{2+}, Al^{3+} and Sr^{2+} ions (samples 1-Mg, 1-Zn, 1-Al, 1-Sr), which were subsequently subjected to firing temperatures at 800, 1000, 1100 and 1200 °C.

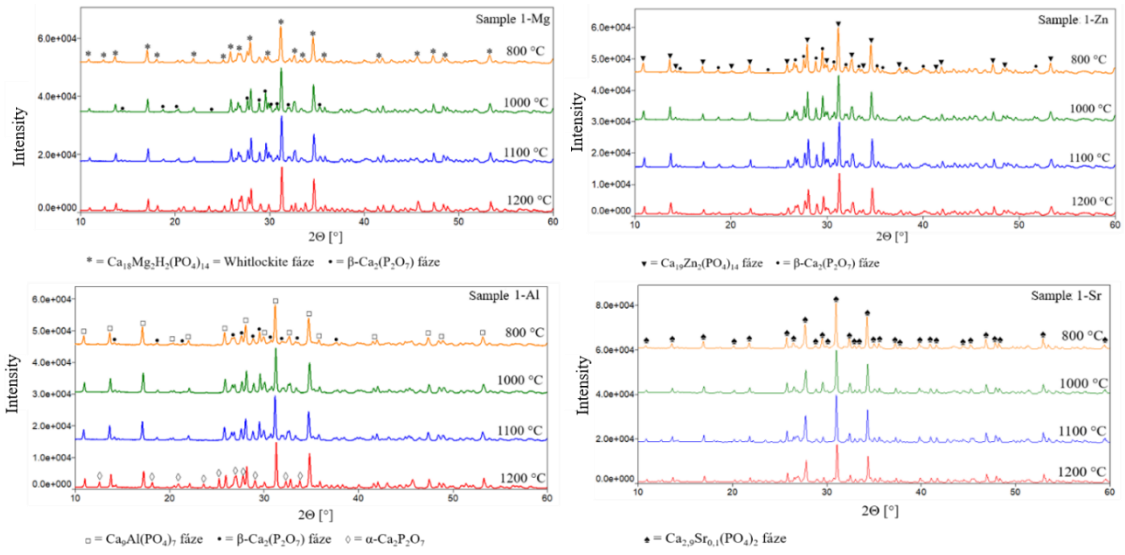

Fig. 6: Phase composition of calcined hydroxyapatite doped with selected ions

From the evaluated diffractograms, it is evident that the calcination process has an influence on the resulting incorporation of the selected ions into the crystal structure of hydroxyapatite. In all samples, the incorporation of the corresponding cation into the structure and the formation of the corresponding compound occurred, as well as the partial phase transformation into β-$Ca_2(P_2O_7)$ and α-$Ca_2P_2O_7$. After substitution with the magnesium cation, the compound $Ca_{18}Mg_2H_2(PO_4)_{14}$, also known as whitlockite was formed, for the zinc cation $Ca_{19}Zn_2(PO_4)_{14}$, for the aluminium cation $Ca_9Al(PO_4)_7$ and for the strontium cation $Ca_{2.9}Sr_{0.1}(PO_4)_2$. This phenomenon is attributed to the fact that these substituted cations (Mg^{2+}, Zn^{2+}, Al^{3+} and Sr^{2+}), whose ionic radii are approximately equal to or smaller than the radius of calcium (r(Ca^{2+}) = 0, 11 nm, r (Mg^{2+}) = 0.072 nm, r (Zn^{2+}) = 0.074 nm, r (Al^{3+}) = 0.054 nm, r (Sr^{2+}) = 0.13 nm) occupied the calcium positions in the hydroxyapatite crystal structure [20, 22, 23].

5.2.3 Scanning electron microscopy of calcinated doped hydroxyapatite powders

The morphology of calcined hydroxyapatite doped pigments was measured using a scanning electron microscope SEM/FIB LYRA 3. Figure 7 shows scanning electron microscope images of the prepared doped HAP pigments at a calcination temperature of 1200 °C.

	Field of view at calcination temperature 1200 °C		
	5 [μm]	10 [μm]	50 [μm]
Sample 1-Mg	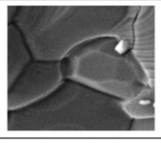	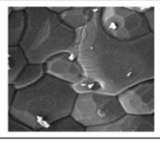	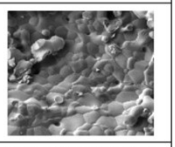
Sample 1-Zn	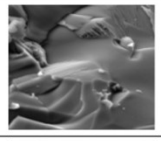	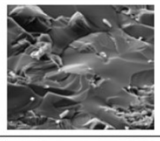	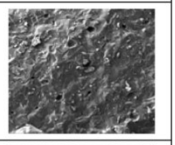
Sample 1-Al	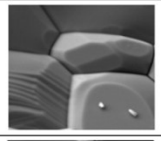	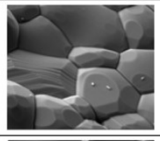	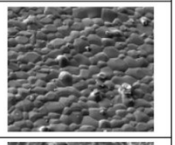
Sample 1-Sr	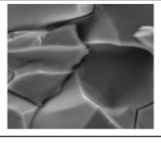	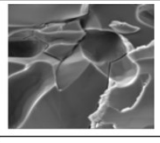	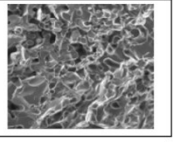

Fig. 7: SEM images of doped hydroxyapatite samples calcinated at 1200 °C

From the SEM images, it can be seen that during the calcination process, the hydroxyapatite particles are gradually compacted with increasing sintering temperature, causing aggregation and the formation of necks between the particles [20, 22, 23].

5.3 Corrosion tests of hydroxyapatite powders

5.3.1 Corrosion performance from preliminary corrosion tests

Preliminary, or interim, corrosion tests included pH and conductivity determination of aqueous pigment suspensions (10%), gravimetric determination of the weight loss of steel plates and the determination of corrosion indicators for steel plates. The purpose of measuring the pH and conductivity of aqueous suspensions of pigments is to stimulate the working laboratory conditions of the pigments. The pH value in the range 7-9 is considered optimal for excellent corrosion inhibition, but in the case of phosphate corrosion pigments, slightly acidic pH values are also acceptable. Conductivity values indicate the concentration of dissociated ion species that are formed as a result of hydrolysis and may be involved in corrosion inhibition processes. Figures 8 and 9 show the change in conductivity and pH values of the pigment suspension over a period of 28 days. The results also include the values obtained for the commercial pigment, ZP-10, which was chosen for the corrosion effect comparison [20, 23].

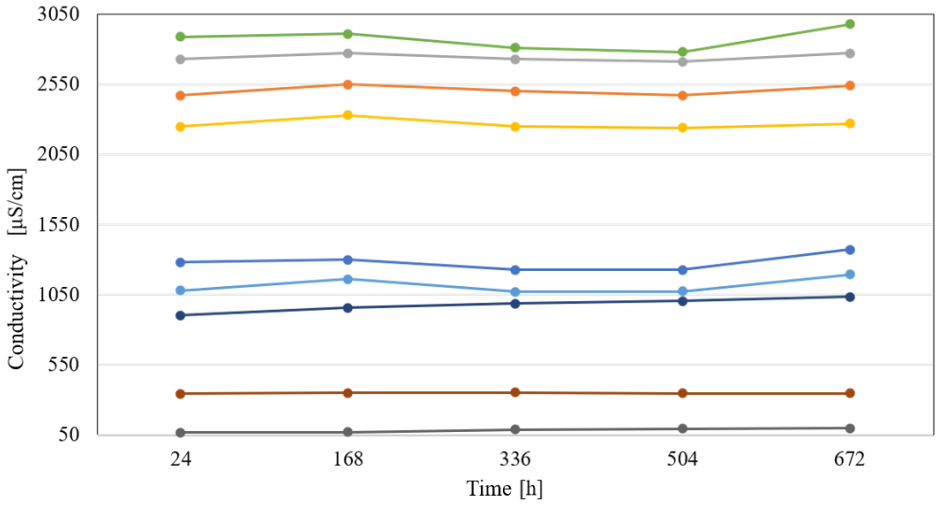

1	1280	1299	1227	1227	1371
1-Mg	2470	2550	2500	2470	2540
1-Zn	2730	2770	2730	2710	2770
1-Al	2250	2330	2250	2240	2270
1-Sr	1080	1162	1071	1074	1195
2	2890	2910	2810	2780	2980
3	903	958	986	1004	1035
4	344	349	354	347	346
ZP-10	68,4	69,9	89	94,7	98,5

Fig. 8: Time dependence of conductivity of aqueous leachates of powdered pigments (28 days)

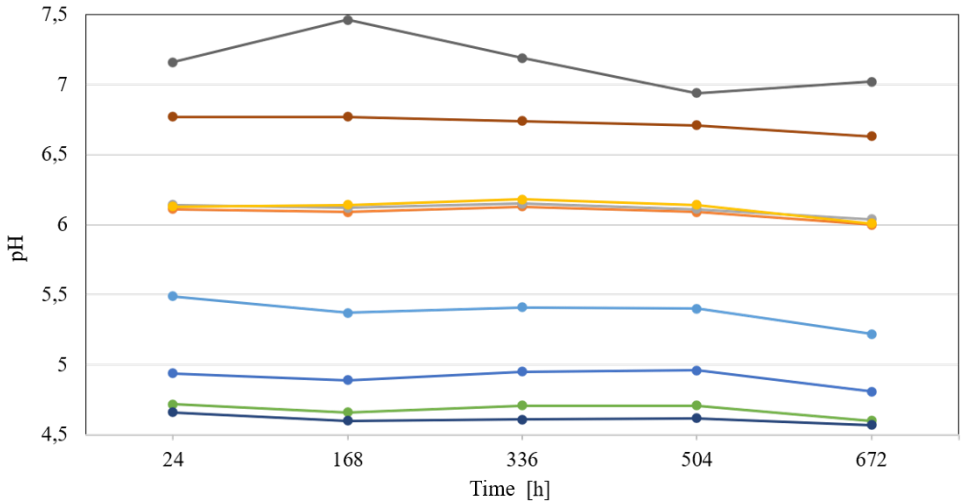

1	4,94	4,89	4,95	4,96	4,81
1-Mg	6,11	6,09	6,13	6,09	6,00
1-Zn	6,14	6,12	6,15	6,11	6,04
1-Al	6,13	6,14	6,18	6,14	6,01
1-Sr	5,49	5,37	5,41	5,40	5,22
2	4,72	4,66	4,71	4,71	4,60
3	4,66	4,60	4,61	4,62	4,57
4	6,77	6,77	6,74	6,71	6,63
ZP-10	7,16	7,46	7,19	6,94	7,02

Fig. 9: Time dependence of the pH value of pigment suspensions (28 days)

Based on the measured values from the preliminary corrosion tests, it was shown that hydrolysis of the pigments favours the formation of acidic ions over basic ions, leading to a decrease in pH values. Conductivity was very different for the samples but generally increased, indicating that the concentration of dissociated ions also increased over time. For most samples (except samples 1-Sr and 4), the high degree of hydrolysis was related to higher surface area and pore volume values. After this test, the suspensions were filtered and the steel plates were immersed in the pigment extracts for 3 months. During the test, a color change of the leachate was visually observed, which is the cause of the exclusion of corrosion products (rust) into the surrounding environment, as well as the formation of corrosion products on the surface of the steel plates. For some of the samples measured, a white coating was observed on the surface of the steel plates, indicating the formation of a phosphate protective coating ($Fe_3(PO_4)_2 \cdot 8H_2O$, vivianite). After the test, corrosion indices were determined based on the relative weight loss of the steel plates. Figure 10 shows the relative corrosion loss values [20, 23].

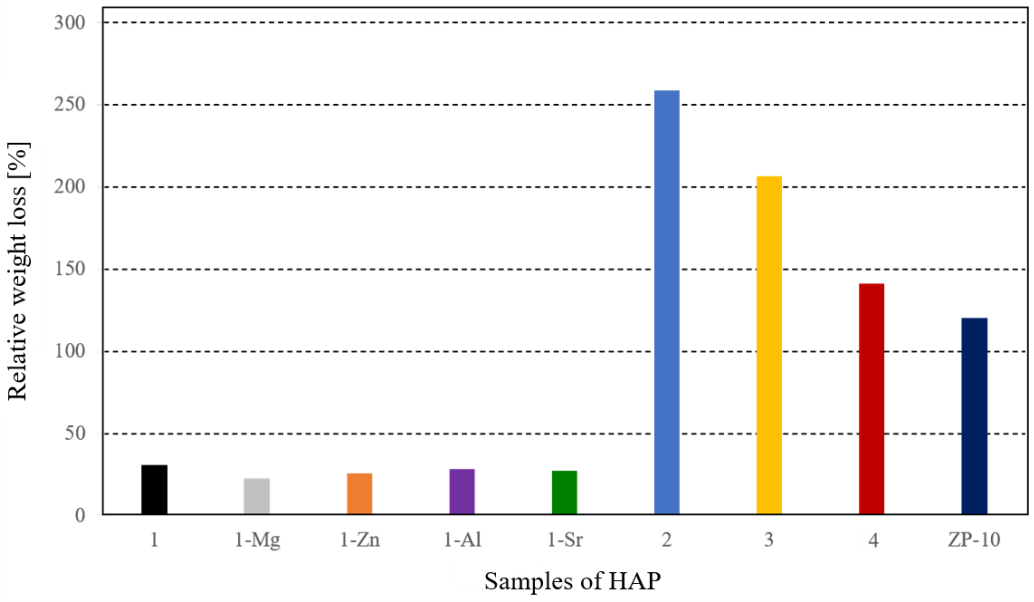

Fig. 10: Relative weight loss of corrosion-prepared samples (water-100 %)

Based on the corrosion indices, the synthesized samples were classified according to their corrosion effectiveness into the following 3 groups.

- Pigments with high anticorrosive efficiency, in whose pigment leachates corrosion processes were decelerated due to high concentration of phosphates, which inhibit corrosion processes. This is related to the medium range of conductivity values (1195-2540 µS/cm) and to the formation of a protective white coating (vivianite, $Fe_3(PO_4)_2 \cdot 8H_2O$) on the surface of the steel plates. Of this group, sample 1-Mg showed excellent corrosion protection properties, which may be related to its two-phase composition (i.e., the whitlockite phase may be more effective for corrosion protection than hydroxyapatite). Thus, the majority of the Series 1 samples (needle-shaped particles) belongs to this group.
- Pigments without anticorrosive properties whose phosphate concentration in the leachates was insufficient for high anticorrosive effectiveness. This is related to the very low conductivity value (98.5-1035 µS/cm) and the formation of the main product of corrosion processes (FeO(OH)). This group includes samples 3, 4 and the commercial pigment ZP-10.
- Pigments promoting corrosion processes, where in the leachates of these samples the corrosion processes were very intense, which can be explained by the strong reaction between the pigment leachate and the steel plate. The conductivity values were high (2770-2980 µS/cm), which caused a substantial deformation of the surface of the plate and the formation of FeO(OH) as the main corrosion product. This can be explained by the presence of hydrated calcium complexes which act as corrosion catalysts. Samples 1-Zn and 2 belong to this group.

Preliminary corrosion tests show that some hydroxyapatite samples demonstrated better corrosion performance than the commercial pigment ZP-10, with up to 2x higher performance in some cases. The corrosion efficiency of the synthesized hydroxyapatite powders is related to the precipitation conditions. That means, the best anticorrosive efficiency was exhibited by samples 1 with needle-shaped particles, where these samples were prepared at Ca/P ratio = 1, pH = 7 with a precipitation rate of 2 $ml \cdot min^{-1}$ [20, 23].

5.3.2 Accelerated corrosion tests

The prepared samples were dispersed in alkyd primer, and the thickness of the dried coatings was checked using a coating thickness gauge. The standard deviation of the coating thickness ranged from 10-20 μm for each sample. Before and after the corrosion test, the color of the samples was measured using the ColorQuest XE and the appearance of the coating was measured using an optical microscope. Evaluation of the degradation of the coatings after the moisture chamber corrosion test was performed with respect to the degree of rusting, blistering, cracking and peeling. The evaluation of the degree of delamination and corrosion in the area around of the cut and on the surface was carried out after coating removal [20, 23].

5.3.2.1 Change in the appearance of the corrosion coatings during the test

After the accelerated corrosion test, the change in the appearance of the corrosion coatings was already visually noticeable. Images of all synthesized samples during the corrosion testing for 3 months are shown in Figure 11. For some of the samples, the corrosion products were more visually visible, with the coating with commercial pigment (ZP-10) showing the best appearance. However, these discolorations may be due to diffusion of corrosion products from the edges of the steel plates where the corrosion stains were very visible. The change in the appearance of the coatings was investigated using a digital optical microscope before and after the corrosion test. Evaluation of these images shows that for all hydroxyapatite samples, the formation of small crystals on the surface of their coating was observed. According to XRD analysis of these crystals obtained, it was shown that they are organic compounds, indicating the destruction of the coating in the corrosion humidity chamber and the formation of corrosion spots with crystals of corrosion products. The exception was the coating surface containing a commercial pigment, which visually showed the least damage and corrosion stains [20, 23].

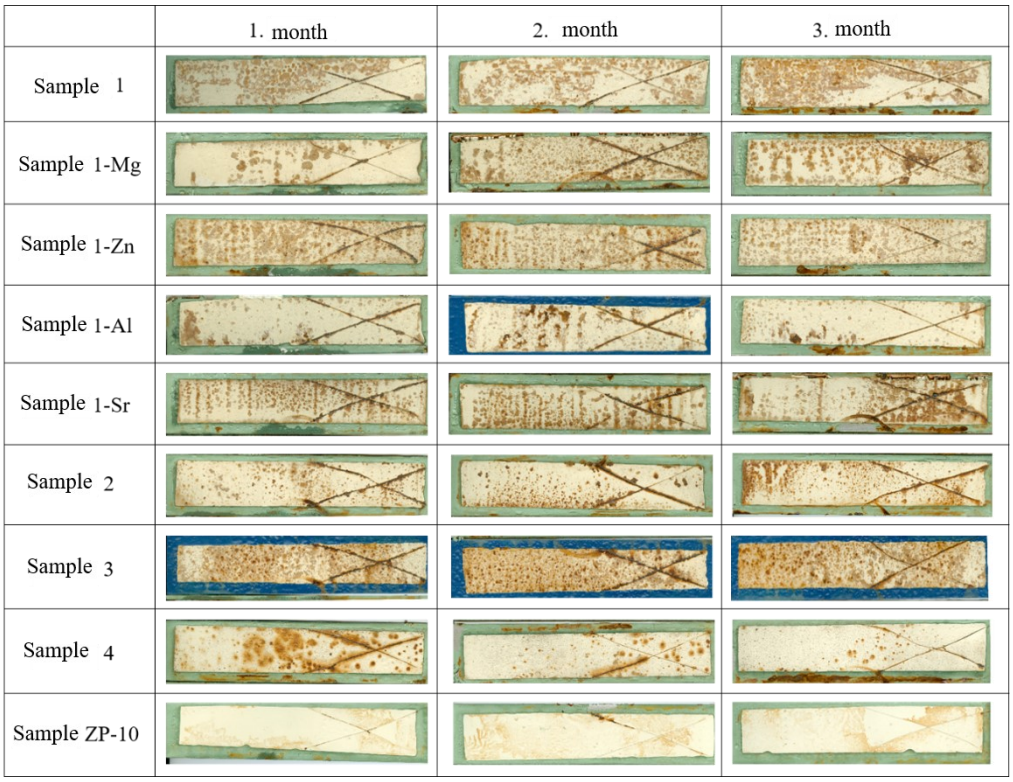

Fig. 11: Appearance of steel plates with coating synthesized samples during corrosion testing for 3 months

The evaluation of the change in the color difference of the coatings before and after the accelerated corrosion test was carried out using a ColorQuest XE spectrophotometer. The values of L^*, a^*, b^* were measured, from which the changes in the overall color difference ΔE^*_{CIE} were subsequently calculated (Table 4). The value of the total color difference makes it possible to express the agreement or disagreement between the sample and the standard on the basis of the numerical interval in which it varies, and therefore gives very important information about the exact nature of the coloration obtained. It is evident from the values of the change in color difference that all the samples reached values higher than 3, so the color difference can be stated to be very significant for all the samples. It can be seen from the ΔE^*_{CIE} values that all samples show a large color difference just after the corrosion test has been carried out, with the commercial standard ZP-10 (ΔE^*_{CIE} = 4.5) and sample 4 (ΔE^*_{CIE} = 7.1) of the prepared samples showing the smallest values, which are still visible to the eye. On the other hand, the highest values were achieved by sample 1-Sr with a color difference change value of 19.7. These results are consistent with the digital optical microscope results [20, 23].

Table 4: Color properties of coatings during accelerated corrosion test

Sample	Before corrosion test			After corrosion test			ΔE^*_{CIE}
	L*	a*	b*	L*	a*	b*	
1	83.5	2.1	19.5	67.7	5.3	16.4	16.5
1-Mg	83.7	1.1	20.1	70.5	5.0	17.7	14.0
1-Zn	81.1	1.4	19.9	68.1	4.7	17.7	13.6
1-Al	86.3	1.3	19.6	74.5	3.0	15.8	12.5
1-Sr	82.0	1.2	18.2	62.7	6.0	17.3	19.7
2	86.0	0.6	17.1	71.4	6.3	20.7	16.1
3	77.1	2.7	18.0	63.0	9.7	22.1	16.3
4	86.1	-0.3	15.3	79.7	1.7	13.3	7.1
ZP-10	85.5	-0.3	15.9	81.8	2.0	15.4	4.5

5.3.2.2 Coating degradation and corrosion on the steel surface

The evaluation of paint degradation after the accelerated corrosion test was carried out according to the relevant standards with respect to color change by subjective observation, degree of blistering, paint rusting, paint cracking, corrosion around the cut and in the paint area. The evaluation of the degree of delamination and corrosion in the around of the cut and in the surface area was carried out after removal of the coating. The results of the evaluation of the aspects studied are presented in Table 5. The surface appearance of the steel plates after subsequent paint removal is shown in Figure 12.

Table 5: Degradation of prepared coatings and evaluation of corrosion in the steel surface area

Sample	Visual color change	Blistering (quantity; size)	Rusting [degree; occurrence of rust, %]	Corrosion	
				Around the cut	In surface area [%]
1	5	4; S_D 4	Ri 4; 8	3	85
1-Mg	5	4; S_D 4	Ri 4; 8	3	80
1-Zn	4	4; S_D 3	Ri 4; 8	2	70
1-Al	3	5; S_D 4	Ri 4; 8	2	75
1-Sr	5	4; S_D 4	Ri 4; 8	5	65
2	4	4; S_D 3	Ri 4; 8	4	50
3	5	5; S_D 4	Ri 5; 40-50	4	85
4	2	4; S_D 3	Ri 3; 1	2	55
ZP-10	1	4; S_D 4	Ri 2; 0,5	1	30

Fig. 12: Appearance of samples after paint removal

In terms of evaluating the subjective visual changes in the color of the paint, all samples showed some intensity of color changes in the top coat (yellowing to browning). Almost all samples showed a very clear or significant color change (classification 3-5) of the topcoat, only two samples, namely 4 and ZP-10 (commercial pigment) showed a very small or just detectable intensity of change (classification 1-2). The amount of blistering was classified as 4 or 5 for all samples, indicating a high number of blisters on the surface of the degraded coating. The size of these blisters can be evaluated by S_D 3 or S_D 4 values, where S_D 3 classification indicates the formation of blisters clearly visible to the eye or with correlated visual defects (up to 0.5 mm) and S_D 4 indicates blister size in the range of 0.5-5 mm. The degree of rusting was classified as Ri 4 for almost all samples, which means that the rust incidence based on the whole measurement area was 8 %. The highest degree of rusting was achieved by sample 3 (Ri 5 classification), where the rust incidence

was 40-50% of the total area. On the other hand, the lowest degree of rusting was achieved by samples 4 and ZP-10 (Ri 2 and Ri 3 classifications), where the total rust coverage based on the total area was 0.5-1 %. The degree of corrosion varied widely between samples. For samples 1, 1-Mg, 1-Zn, 1-Al, 4 and ZP-10, the degree of corrosion was classified in the range of values 1-3, indicating a very slight to moderate degree of corrosion. On the other hand, samples 1-Sr, 2 and 3 exhibited a corrosion degree with values of 4 and 5, indicating a significant to very significant degree of corrosion. The assessment of corrosion in the surface area of the samples was done visually and the percentage ranges from 30-85 %. The highest percentage of corrosion in the surface area was observed in samples 1 and 3 (85 %) and on the contrary the lowest was for the standard sample ZP-10 (30 %).

In general, the lowest color change, degree of rusting, blistering, cracking and corrosion in section and surface area was observed for the commercial pigment ZP-10. Thus, from the results obtained and evaluated for the synthesized pigments, it can be concluded that under the given conditions, samples 1-Al and 4 exhibit better anticorrosion properties. The poor anticorrosion properties of samples 1 and 3 are related to the results of paint appearance change, color difference and also to the results of preliminary corrosion tests.

6 CONCLUSION

The main objectives of this dissertation work were focused on the research and evaluation of the effect of selected synthesis precipitation conditions (Ca/P ratio, pH, precipitation rate) for the preparation of hydroxyapatite powder materials, their subsequent calcination at firing temperatures of 800, 1000, 1100 and 1200 °C. This was followed by the study of partial substitution of calcium ions in the hydroxyapatite structure by other selected elements (magnesium, zinc, aluminium, strontium) and subsequent evaluation of their possible adaptation in the hydroxyapatite structure. One of the other objectives was to characterize and describe the physicochemical properties of the pure and doped hydroxyapatite phase by available laboratory techniques. The final objective was to verify and subsequently evaluate the influence of precipitation conditions and partial substitution by other elements on the corrosion inhibitory effects of hydroxyapatite.

From the particle size distribution analyses, it was found that the results of undoped and doped samples correspond to the size of agglomerates. The narrowest particle size distribution was obtained for undoped sample 1, while doping the sample caused the range of particle size distribution to widen. Sample 1-Mg showed the narrowest range of particle size distribution under substitution, which may be related to the results from XRD analysis, where its biphasic composition was demonstrated, as whitlockite was identified along with hydroxyapatite. The narrow range of particle size distribution is very significant for further studies of hydroxyapatite in terms of its anticorrosion effectiveness as a corrosion inhibitor.

From the results of XRD analyses, it was evident that two distinct structures of hydroxyapatite were identified for the undoped samples, namely monoclinic (crystallographic system with space group $P2_1/b$) and hexagonal (crystallographic system with space group $P6_3/m$). For most doped samples only a single phase composition was demonstrated, as for undoped samples, but only one doped element (Mg, sample 1-Mg, $Ca_{9.5}Mg_{0.5}(PO_4)_6(OH)_2$) contained two phases, namely hydroxyapatite $Ca_{10}(PO_4)_6(OH)_2$ and whitlockite $Ca_{18}Mg_2H_2(PO_4)_{14}$. As only the hydroxyapatite phase was identified in the other doped samples, it was clear that

these doped ions (Zn^{2+}, Al^{3+} and Sr^{2+}) probably occupied the calcium positions in the hydroxyapatite crystal structure. This was expected because the ionic radii of these substituted ions are approximately as large as or smaller than the radius r (Ca^{2+}) = 0.11.

Interesting findings were also obtained in terms of calcination of all the synthesized samples which were subjected to PSD, XRD and SEM analyses after this process.

From the width of the particle size distribution of all the synthesized samples, it was concluded that during the calcination process, the number of small particles in the total volume decreases, resulting in the formation of agglomerates of larger particles, which is consistent with the width of the distribution curve moving towards higher values.

From the diffractograms obtained from XRD analyses, it was found that the calcination process has an effect on the final phase composition of the synthesized undoped samples. The same phases were identified for samples 1, 2 and 4, namely whitlockite (at 800-1100 °C) and α-$Ca_3(PO_4)_2$ (only at 1200 °C). This suggests that at firing temperatures of 800, 1000 and 1100 °C the hydroxyapatite phase transforms to the more stable whitlockite phase, whereas at higher firing temperatures (1200 °C) the subsequent and complete transformation to α-$Ca_3(PO_4)_2$, the final product of hydroxyapatite decomposition occurs and is also evident from the thermal analysis results obtained. From the evaluated diffractograms of the doped samples, it was shown that the calcination process has an influence on the resulting incorporation of the selected ions into the crystal structure of hydroxyapatite. In all samples, the incorporation of the corresponding cation into the structure, the formation of the corresponding compound and the partial phase transformation to β-$Ca_2(P_2O_7)$ and α-$Ca_2P_2O_7$ occurred.

From SEM analyses of undoped and doped samples, it was shown that the sintering of hydroxyapatite particles occurs during the calcination process. During this process, a gradual densification of the hydroxyapatite particles occurred with increasing sintering temperature, causing agglomeration and the formation of necks between the particles.

Therefore, based on the results of all the analyses performed, it can be concluded that the selected synthesis conditions are suitable for the formation of crystalline hydroxyapatite. For this reason, undoped samples 1, 2, 3, 4 and doped samples 1-Mg, 1-Zn, 1-Al and 1-Sr were selected for further research, which was aimed at verifying the anticorrosion effects.

Based on the results of the preliminary corrosion tests, the samples were classified according to their corrosion effectiveness into the following 3 groups.

- The first group includes samples with high corrosion efficiency, which form a protective white coating on the surface of the steel plates. From this group, sample 1-Mg showed excellent anticorrosion properties, which may be related to its two-phase composition (whitlockite and hydroxyapatite).
- The second group involves samples without anticorrosion properties, which led to the formation of the main corrosion product FeO(OH). Samples 3, 4 and the commercial pigment ZP-10 belong to this group.
- The third group covers samples that are conducive to corrosion processes. This can be explained by the presence of hydrated calcium complexes which act as corrosion catalysts. Samples 1-Zn and 2 belong to this group.

Preliminary corrosion tests therefore show that some hydroxyapatite samples demonstrated better corrosion effectiveness than the commercial pigment ZP-10, with some cases showing up to 2x higher effectiveness. The corrosion efficiency of the synthesized hydroxyapatite powders is related to the precipitation conditions. That is, the best anticorrosive efficiency was exhibited by samples 1 with needle shaped particles, where these samples were prepared at Ca/P ratio = 1, pH = 7 with a precipitation rate of 2 $ml \cdot min^{-1}$. However, no correlation between anticorrosive efficiency, surface area and porosity was shown, indicating that in the case of synthesized hydroxyapatite, its chemical properties (surface activity) are preferred over its physical properties. This result may be related to the high degree of hydrolysis of hydroxyapatite and the formation of a large number of ions (at lower solubility, the physical properties would dominate).

In the next stage, accelerated corrosion tests of the pigment coatings were carried out using a humidity corrosion chamber. Based on the results from the accelerated corrosion tests, the prepared pigments were dispersed in an alkyd primer. Before and after the corrosion test, the color of the samples was measured and the appearance of the coating was observed. The evaluation of the degradation of the coatings after the corrosion test was carried out according to the relevant standards with respect to the degree of rusting, blistering, cracking and peeling. The evaluation of the degree of delamination and corrosion in the vicinity of the cut and on the surface was carried out after removal of the coating. The commercial pigment ZP-10 showed the best result with respect to color change, degree of rusting, blistering, cracking and corrosion in the cut and surface area. From the results obtained and evaluated for the synthesized samples, it is evident that samples 1-Al and 4 showed better anticorrosion properties, while samples 1 and 3 showed significantly worse anticorrosion properties.

Based on the tests performed and the results obtained for the prepared samples to verify the anticorrosion performance in the alkyd coating, it was found that these samples did not achieve adequate anticorrosion performance compared to the commercial pigment ZP-10. For further research, it would be advisable to verify the application in a different coating, or to check the possibility of surface treatment of the prepared powders to see if their anticorrosive efficiency could be improved.

7 LIST OF REFERENCES

[1] MYŠKOVÁ V., *Syntéza a vlastnosti fosforečnanů dopovaných prvky vzácných zemin*. Pardubice, 2014. Disertační práce. Univerzita Pardubice.

[2] ŠUSTEK, S., *Testování korozně-inhibičních účinků pigmentů na bázi orthofosforečnanů*. Pardubice, 2009. Diplomová práce. Univerzita Pardubice.

[3] KALENDOVÁ A., *Technologie nátěrových hmot I.: pigmenty a plniva pro nátěrové hmoty*. Pardubice: Univerzita Pardubice, 2003. ISBN 80-719-4576-5.

[4] KALENDA P. a VESELÝ D., *Koroze a protikorozní ochrana kovových materiálů*. Pardubice: Univerzita Pardubice, 2003. ISBN 80-719-4600-1.

[5] SLEPKO A., *Theory of biomineral hydroxyapatite.* 2013.

[6] YAEMSUNTHORN K., RANDORN C., *International Journal of Hydrogen Energy*. 2017, **42**, 5056.

[7] SHEPHERD J. H., SHEPHERD D. V. a BEST S. M., Substituted hydroxyapatites for bone repair. *Journal of Materials Science: Materials in Medicine*. 2012, **23**(10), 2335-2347. ISSN 0957-4530. Dostupné z: doi:10.1007/s10856-012-4598-2.

[8] DOBOŠ P., *Příprava biokeramických materiálů pro medicínské aplikace*. Brno, 2010. Bakalářská práce. VUT, Fakulta chemická, Ústav chemie materiálů.

[9] STANIC V., Synthesis of fluorine substituted hydroxyapatite nanopowders and application of the central composite design for determination of its antimicrobial effects. *Applied Surface Science*. 2014, (290), 346-352. Dostupné z: doi:doi.org/10.1016/j.apsusc.2013.11.081.

[10] MERRY J. C., GIBSON I. R., BEST S. M. a BONFIELD W., Synthesis and characterization of carbonate hydroxyapatite. *Journal of Materials Science: Materials in Medicine*. 1998, **9**(12), 779-783. ISSN 0957-4530. Dostupné z: doi:10.1023/A:1008975507498.

[11] RIVERA-MUNO, E., Hydroxyapatite-Based Materials: Synthesis and Characterization. *Biomedical Engineering - Frontiers and Challenges*. InTech, 2011, 2011-08-01. ISBN 978-953-307-309-5. Dostupné z: doi:10.5772/19123.

[12] DOROZHKIN S. V., Bioceramics of calcium orthophosphates. *Biomaterials*. 2010, **31**(7), 1465-1485. ISSN 01429612. Dostupné z: doi:10.1016/j.biomaterials.2009.11.050.

[13] KAY M. I., YOUNG R. A. a POSNER A. S., Crystal Structure of Hydroxyapatite. *Nature*. 1964, **204**(4963), 1050-1052. ISSN 0028-0836. Dostupné z: doi:10.1038/2041050a0.

[14] Calcium Orthophosphates: Crystallization and Dissolution. PMC. *Www.ncbi.nlm.nih.gov* [online]. 2009 [cit. 2020-9-22]. Dostupné z: http://www.ncbi.nlm.nih.gov/pmc/articles/PMC2743557.

[15] SÁENZ A., RIVERA-MUÑOZ E. a BROSTOW W., Ceramic biomaterials: an introductory overview. *Journal of Materials Education*. 1999, (21), 297 – 306.

[16] GORODYLOVA N., DOHNALOVÁ Ž., ŠULCOVÁ P., BĚLINA P. a VLČEK M., Influence of synthesis conditions on physicochemical parameters and corrosion inhibiting activity of strontium pyrophosphates SrMIIP2O7 (MII = Mg and Zn). *Progress in Organic Coatings*. 2016, **93**, 77-86. ISSN 03009440. Dostupné z: doi:10.1016/j.porgcoat.2016.01.004.

[17] ŠIMKOVÁ L., *Vliv podmínek srážení na syntézu hydroxyapatitu a jeho korozně inhibiční vlastnosti*. Pardubice, 2017. Diplomová práce. Univerzita Pardubice.

[18] PŘIBIL R., *Komplexometrie: určeno technikům se středním vzděláním a studentům průmyslových škol*. Praha: Státní nakladatelství technické literatury, 1961. Řada chemické literatury.

[19] ŠIMKOVÁ L., GORODYLOVÁ N., DOHNALOVÁ Ž., ŠULCOVÁ P., Influence of precipitation conditions on the synthesis of hydroxyapatite, *Ceramics and Silikáty*. 2018, **62**, 253-260. ISSN 1804-5847. Dostupné z: doi:10.13168/cs.2018.0019.

[20] ŠIMKOVÁ L. a ŠULCOVÁ P., Magnesium, aluminum and zinc co-substituted hydroxyapatite: anti-corrosion properties. *Anti-Corrosion Methods and Materials.* 2019, **66**(4), 496-506. ISSN 0003-5599. Dostupné z: doi:10.1108/ACMM-11-2018-2029.

[21] ŠIMKOVÁ L. a ŠULCOVÁ P., Characterization and thermal behavior of hydroxyapatite prepared by precipitation. *Journal of Thermal Analysis and*

Calorimetry. 2019, **138**(1), 321-329. ISSN 1388-6150. Dostupné z: doi:10.1007/s10973-019-08144-5.

[22] ŠIMKOVÁ L., ŠULCOVÁ P., The effect of calcination on the hydroxyapatite structure. *Scientific Papers University of Pardubice, Series A: Faculty of Chemical Technology*. 2019, **25**, 75-82. ISBN 978-80-7560-243-5.

[23] ŠIMKOVÁ L., ŠULCOVÁ P., The effect of partial substitution on the hydroxyapatite properties. *Scientific Papers University of Pardubice, Series A: Faculty of Chemical Technology*. 2020, **26**, 235-243. ISBN 978-80-7560-322-7.

8 LIST OF STUDENT'S PUBLISHED WORK

8.1 RESEARCH PUBLICATIONS

Šimková Lenka, Gorodylová Nataliia, Dohnalová Žaneta, Šulcová Petra: Influence of precipitation conditions on the synthesis of hydroxyapatite. *Ceramics and Silikáty*. 2018, **62**, 253-260.

Šimková Lenka, Šulcová Petra: Magnesium, aluminum and zinc co-substituted hydroxyapatite: anti-corrosion properties. *Anti-Corrosion Methods and Materials*. 2019, **66**, 496-506.

Šimková, Lenka, Šulcová Petra: Characterization and thermal behavior of hydroxyapatite prepared by precipitation. *Journal of Thermal Analalysis and Calorimetry*. 2019, **138**, 321–329.

Šimková Lenka, Šulcová Petra: The effect of calcination on the hydroxyapatite structure. *Scientific Papers University of Pardubice, Series A: Faculty of Chemical Technology*. 2019, **25**, 75-82.

Šimková Lenka, Šulcová Petra: The effect of partial substitution on the hydroxyapatite properties. *Scientific Papers University of Pardubice, Series A: Faculty of Chemical Technology*. 2020, **26**, 235-243.

8.2 LECTURE AND POSTER

Šimková Lenka, Gorodylova Nataliia, Šulcová Petra: *Influence of precipitation conditions on the synthesis of hydroxyapatite* (**lecture**). Chémia a technológie pre život-19. celoslovenská študentská vedecká konferencia s medzinárodnou účasťou, Bratislava 09.11.2017, s. 78-79, ISBN 978-80-89579-77-2.

Šimková Lenka, Gorodylová Nataliia, Dohnalová Žaneta, Šulcová Petra: *Vliv podmínek srážení na syntézu hydroxyapatitu a jeho antikorozní vlastnosti* (**lecture**), Anorganické nekovové materiály – odborný seminář doktorandů, Praha 07-08.02.2018, s. 13.

Šimková Lenka, Gorodylová Nataliia, Dohnalová Žaneta, Šulcová Petra: *Sytnhtesis and characterization of hydroxyapatite for anticorrosion purposes* (**poster**), 6th International Conference on Chemical Technology, Mikulov 16-18.04.2018, s. 1-4, ISBN 978-80-86238-83-8.

Šimková Lenka, Gorodylova Nataliia, Šulcová Petra: *Využití hydroxyapatitu substituovaného prvky Mg, Zn, Al jako inhibitoru koroze* (**poster**), Moderné TRENDY v anorganických technologiích 2018, Bánská Štiavnica 21.-23.05.2018, s. 34-35, ISBN 978-80-7592-016-4.

Vaško Patrik, Šimková Lenka, Šulcová Petra: *Příprava směsných oxidických pigmentů* (**lecture**), Studentská vědecká odborná činnost, Pardubice 11.06.2018, s. 193-198, ISBN 978-80-7560-157-5.

Šimková Lenka, Šulcová Petra: *Thermal behavior of hydroxyapatite* (**poster**),13th Conference on Calorimetry and Thermal Analysis of the Polish Society of Calorimetry and Thermal Analysis, Zakopane,Polsko 02-06.09.2018, s. 148.

Šimková Lenka, Šulcová Petra: *Synthesis, thermal stability and corrosion properties of pure and substituted hydroxyapatite* (**poster**), 13th International Conference on Solid State Chemistry, Pardubice 16-21.09.2018, s. 143, ISBN 978-80-7560-158-2.

Šimková Lenka, Šulcová Petra: *The impact of Ca/P ratio and pH on synthesis of hydroxyapatite and its thermal behaviour* (**poster**), 20. ročník Konference o Speciálních anorganických pigmentech a práškových materiálech, Pardubice 19.09.2018, s. 92-97, ISBN 978-80-7560-145-2.

Šimková Lenka, Šulcová Petra: *Synthesis and thermal stability of hydroxyapatite* (**lecture**), Chémia a technológie pre život – 20. celoslovenská študentská vedecká konferencia s medzinárodnou účasťou, Bratislava 07.11.2018, s. 59-60, ISBN 978-80-89579-99-4.

Šimková Lenka, Šulcová Petra: *Synthesis and characterization of HAP powders by precipitation method* (**lecture**), Odborný seminář doktorandů – Anorganické nekovové materiály, Praha – Česká republika, 6. – 7. 2. 2019, s. 18-19.

Šimková Lenka, Šulcová Petra: *The effect of firing temperatures on the structure of hydroxyapatite* (**poster**), 7. mezinárodní chemicko-technologická konference, Mikulov – Česká republika, 15. – 17. 4. 2019. P17 – rozsah 1 strana. ISBN: 978-80-88307-01-3.

Šimková Lenka, Luxová Jana: *Influence of raw materials on optical properties of Bi-doped $PrFeO_3$* (**poster**), 7. mezinárodní chemicko-technologická konference, Mikulov – Česká republika, 15. – 17. 4. 2019. P18 – rozsah 1 strana. ISBN: 978-80-88307-01-3.

Hofmanová Tereza, Šimková Lenka, Šulcová Petra: *Vliv způsobu přípravy na barevné vlastnosti sloučeniny typu Bi-Tb-Ce, Sb* (**lecture**). Studentská vědecká odborná činnost, Pardubice, 10.06.2019, s. 47-52, ISBN 978-80-7560-260-2.

Šimková Lenka, Šulcová Petra: *Characterization of thermal behavior of pure and doped hydroxyapatite* (**poster**), 2nd Journal of Thermal Analysis and Calorimetry Conference, Budapešť – Maďarsko, 18. – 21. 6. 2019, 569, ISBN 978-963-454-416-6.

Šimková Lenka, Šulcová Petra: *The hydroxyapatite and its anti-corrosion properties* (**poster**), XIII. International Conference Preparation of Ceramic Materials, Košice – Jahodná – Slovensko, 25. – 27. 6. 2019, 184-185, ISBN 978-80-553-3314-4.

Šimková Lenka, Šulcová Petra: *Influence of partial substitution of selected elements on the structure and properties of HAP* (**lecture**), 21. Konference o speciálních anorganických pigmentech a práškových materiálech, Pardubice – Česká republika, 18. 9. 2019, str. 48–53, ISBN 978-80-7560-222-0.

Šimková Lenka, Šulcová Petra: *Study of hydroxyapatite by thermal analysis methods* (**poster**), Termoanalytický seminář, Brno – Česká republika, 10. 10. 2019, s. 142-147, ISBN 978-80-88307-03-7.

Hofmanová Tereza, Šimková Lenka, Šulcová Petra: *Vliv způsobu přípravy na barevné vlastnosti oxidického pigmentu* (**lecture**), Chémia a technológie pre život – 21. celoslovenská študentská vedecká konferencia s medzinárodnou účasťou, Bratislava 06.11.2019, s. 69-70, ISBN 978-80-8208-015-8.

Šimková Lenka, Šulcová Petra: *The effect of substitution on properties and structure of hydroxyapatite* (**lecture**), Odborný seminář doktorandů – Anorganické nekovové materiály, Praha – Česká republika, 12. 2. 2020, s. 10-11.

Šimková Lenka, Šulcová Petra: *The synthesis, characterization and anti-corrosive properties of doped hydroxyapatite* (**lecture**), 22. Konference o speciálních anorganických pigmentech a práškových materiálech, Pardubice – Česká republika, 24. 9. 2020, s. 44-48, ISBN 978-80-7560-296-1.